IOSR Journal Of Applied Physics (IOSR-JAP)
e-ISSN: 2278-4861.Volume 13, Issue 4 Ser. I (Jul. – Aug. 2021), PP 24-38
www.Iosrjournals.Org

Statistical Analysis of Data-set of Groundwater Locations of a 4 km^2 VES Data-field at the Southern Phase II Development, Gidan Kwano Campus, Minna, Nigeria

Jonah, S.A., Akintayo, A.A., Adebayo, H.M., Adegboye, J.A., Mohammed, A.A., and Obagbemi, S.D.
Department of Physics, Federal University of Technology, Minna, Nigeria

Abstract
A limited-extent test of the validity of using a statistical tool in conjunction with acquired ground electrical resistivity data to build a protocol that could ease the efforts and cost that is put into acquiring labourious vertical electrical sounding (VES) data-field in a geologically-similar locality has been completed at the 4 km^2 southern Phase II Development of the Gidan Kwano Campus, Minna, Nigeria. The arbitrarily-fixed very high correlation threshold chosen for that study ensured that the statistical tool under consideration was given a negative recommendation even though the fundamental mathematics of this method was sound and the prevailing geology was encouraging. The aim of this study is to expand the scope of that previous study so as to further examine the results of the simple regression analysis (SRA) method as applied to the corpus of the 4 km^2 VES data-field for a more agreeable or flexible value of correlation threshold; the key objective of this study is achieved by setting the correlation threshold at the median boundary point of 50%. For each groundwater-prospect location, a table of acquired dependent variables (that is, resistivity values) for particular values of the independent variables (that is, AB/2, the current-electrode spacing) was drawn up; such a table is the "x and y table" where x corresponds to AB/2 and y corresponds to the appropriate column of resistivity values. Furthermore, the necessary statistical parameters associated with the SRA method were computed for each table. Subsequently, tables of correlations for the 57 definite groundwater prospect locations down to the 100 m depth-mark and down to the 40 m depth-mark were computed. Based on the "fair boundary point" threshold correlation of 50% used for this study, against the "tough boundary point" of 75% that was set for the previous study, a 42/57th or 73.684% positive correlation for y and y^1 of groundwater prospect locations down to 100 m for the 57 definite groundwater prospect locations means that the reliability of the simple regression analysis route is sufficiently excellent to be trusted. Also, based on this 50% threshold correlation, a 42/57th or 73.684% positive correlation for y and y^1 of groundwater prospect locations down to 40 m for the 57 definite groundwater prospect locations means that the simple regression analysis route can be used as a cost-cutting routine whereby maximum depths of survey of intervening prospect locations should be limited to just this 40 m, and then other values downward would be appropriately predicted before inputting into any purpose-specific interpretation software.

Keywords: VES; resistivity; groundwater; statistical-analysis; SRA

Date of Submission: 13-07-2021 Date of Acceptance: 29-07-2021

I. Introduction

The work of Jonah *et al.* (2018B) was a limited-extent test of the validity of using a statistical tool in conjunction with acquired ground electrical resistivity data to build a protocol that could ease the efforts and cost that is put into acquiring labourious vertical electrical sounding (VES) data-field in a geologically-similar locality. The analytical basis for Jonah *et al.* (2018B) was Jonah and Olasehinde (2017); the arbitrarily-fixed very high correlation threshold chosen for Jonah *et al.* (2018B) ensured that the statistical tool under consideration was given a negative recommendation even though the fundamental mathematics of this method was sound and the prevailing geology was encouraging. The method of simple regression analysis shows the relationship between an independent and a dependent variable, as well as providing a means for the derivation of an equation to predict the dependent variable based on the values of the independent variable (Morenikeji, 2006). The regression equation is expressed as

$$y^1 = a + bx \qquad 1$$

In Eq.1, y^1 is the predicted value of the dependent variable for any particular value of x, the independent variable. Before Eq.1 can be used the values of a and b (constants) have to be determined from the data-set under analysis. Generally,

$$a = \bar{y} - b\bar{x} \quad (2)$$

and

$$b = \frac{n(\Sigma xy) - (\Sigma x)(\Sigma y)}{n(\Sigma x^2) - (\Sigma x)^2} \quad (3)$$

In Eq.2, $\bar{y}$ is the mean of the sum of the different values of y, while $\bar{x}$ is the mean of the sum of the different values of x. Usually, a table of values is produced so that the values of Σx, Σy, Σxy, Σx^2, and $(\Sigma x)^2$, as seen from Eq.3, can easily be computed. It is instructive to point out that in Eq.3, n is the total number of distinct values of the dependent or independent variable.

Loke (2001) stated that the purpose of electrical surveys is to determine the subsurface resistivity distribution by making measurements on the ground surface. The ground resistivity is related to various geological parameters such as the mineral and fluid content, porosity, and degree of water saturation in the rock. Electrical resistivity surveys have been used for many decades in hydrogeological, mining, and geotechnical investigations; its recent application is its use in environmental surveys. The author stated further that the fundamental physical law used in resistivity surveys is Ohm's law that governs the flow of current in the ground. The equation for Ohm's law in vector form for current flow in a continuous medium is given by

$$\mathbf{J} = \sigma \mathbf{E} \quad (4)$$

where σ is the conductivity of the medium, $\mathbf{J}$ is the current density and $\mathbf{E}$ is the electric field intensity. In practice, what is measured is the electric field potential. The author pointed out also that in geophysical surveys the medium resistivity, ρ, which is equals to the reciprocal of the conductivity ($\rho = 1/\sigma$), is more commonly used. The relationship between the electric potential and the field intensity is given by

$$\mathbf{E} = -\nabla\Phi \quad (5)$$

Combining Eqs 1 and 2, we get

$$\mathbf{J} = -\sigma\nabla\Phi \quad (6)$$

In almost all surveys, the current sources are in the form of point sources. In this case, over an elemental volume ΔV surrounding the current source I, located at (x_s, y_s, z_s) the relationship between the current density and the current (Dey and Morrison, 1979) is given by

$$\nabla.\mathbf{J} = \frac{I}{\Delta V}\delta(x - x_s)\delta(y - y_s)\delta(z - z_s) \quad (7)$$

where δ is the Dirac delta function. Eq. 4 can then be rewritten as

$$-\nabla \bullet[\sigma(x, y,z)\nabla\varphi(x, y,z)] = \frac{I}{\Delta V}\delta(x - x_s)\delta(y - y_s)\delta(z - z_s) \quad (8)$$

This is the basic equation that gives the potential distribution in the ground due to a point current source. A large number of techniques have been developed to solve this equation. This is the "forward" modeling problem, that is, to determine the potential that would be observed over a given subsurface structure. Fully analytical methods have been used for simple cases, such as a sphere in a homogenous medium or a vertical fault between two areas each with a constant resistivity. For an arbitrary resistivity distribution, numerical techniques are more commonly used. For the 1-D case, where the subsurface is restricted to a number of horizontal layers, the linear filter method is commonly used (Koefoed, 1979). For 2-D and three-dimensional (3-D) cases, the finite-difference and finite-element methods are the most versatile. Akca (2016) posited that Mufti (1976), Dey and Morrison (1979a; 1979b) discussed the finite-difference approach whilst Coggon (1971), Rijo (1977), Pelton *et al.* (1978) discussed the finite-element approach.

The Phase II Development is an 8 km² swath of land of the Gidan Kwano Campus, Federal University of Technology, Minna, that is ideal for the University's near-term and mid-term facility expansion programmes (Jonah and Olasehinde, 2015; Jonah *et al.*, 2015A; Jonah *et al.*, 2015B; Jonah *et al.*, 2015C; Jonah *et al.*, 2015D; Jonah, 2016; Jonah and Jimoh, 2016; Jonah and Saidu, 2016; Jonah and Olasehinde, 2017; Jonah and Adamu, 2017; Jonah and Abdulrasheed, 2018; Jonah *et al.*, 2018A; Jonah *et al.*, 2018B; Jonah and Saidu, 2018C; Jonah and Saidu, 2018D; Jonah and Saidu, 2018E). On the ground, this 8 km² areal extent is a perfect rectangle with its ends corresponding to the following georeferenced co-ordinates: $9^0$33′07.4″N, $6^0$25′39.0″E (most extreme northwest); $9^0$33′07.4″N, $6^0$26′43.8″E (most extreme northeast); $9^0$30′57.8″N, $6^0$25′39.0″E (most extreme southwest); $9^0$30′57.8″N, $6^0$26′43.8″E (most extreme southeast). Accurate traverse fixing is desirable to build a grid for the 8 km² swath and georeferencing of survey stations is desirable to independently verify the results of this study. At 100 m separation, a total of 21 profile lines were identified in the longitudinal traverse sense and a total of 41 profile lines were identified in the transverse traverse sense. This traverse fixing scheme results in 21 x 41 = 861 principal survey stations. Station-designation format for this survey follows a two-dimensional spatial awareness: principal profile lines are in the north-south direction, with the first profile line being the westernmost line of longitude; numerical station-designation is from west to east. Thus, the first assigned station of survey based on this format is the most extreme southwestern point in the 4 km by 2 km grid appropriately

called P1-1; that is, Station 1 of Profile 1. Station 2 of Profile 1 (P1-2) is exactly 100 m to the north of Station 1; Station 3 of Profile 1 (P1-3) is exactly 100 m to the north of Station 2 and exactly 200 m north of Station 1, and so on. P2-1 means Station 1 of Profile 2; this is exactly 100 m to the east of P1-1; P3-1 is exactly 100 m to the east of P2-1 and exactly 200 m to the east of P1-1. Each of these principal survey stations was visited whence its latitude, longitude, and elevation information (x, y, z) were measured and duly recorded. On the ground, against the backdrop of a satellite imagery map showing Phase I (obviously, the present developed portion), the locations of the principal stations are as shown in Figure 1.

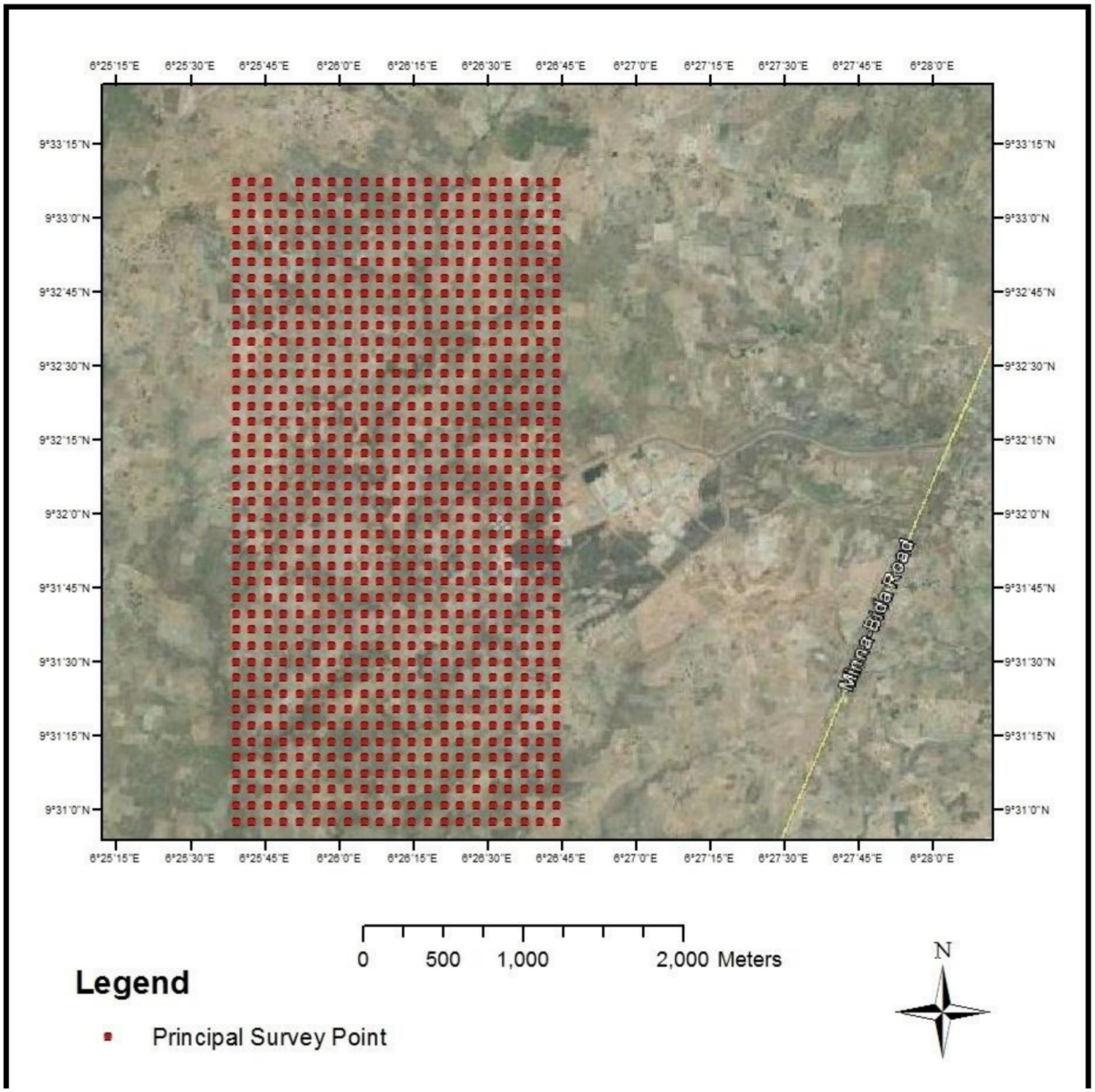

Figure 1. Locations of the principal stations against the backdrop of a satellite imagery map showing Phase I

The southern 4 km^2 areal extent at the Phase II Development of the Gidan Kwano Campus where a full-body VES study was completed (Jonah and Olasehinde, 2017) is shown as Figure 2. There are 441 principal stations in the grid of Figure 2: not all the 441 principal survey stations of the 4 km^2 areal extent were occupied during the course of the VES survey because of barriers encountered at coincident points of surveys; the barriers are those due to wet-stream, outcrop, thicket, built-up area, instrumental error (that is, "Error 12" of the ABEM Terrameter 4000), and raw sewage. The schedule of Figure 2 has been colour-coded to indicate the stations that were occupied for data collection during the course of this survey, see Figure 3. The pattern of field VES data collection for the work of Jonah and Olasehinde (2017) was a transverse traverse format.

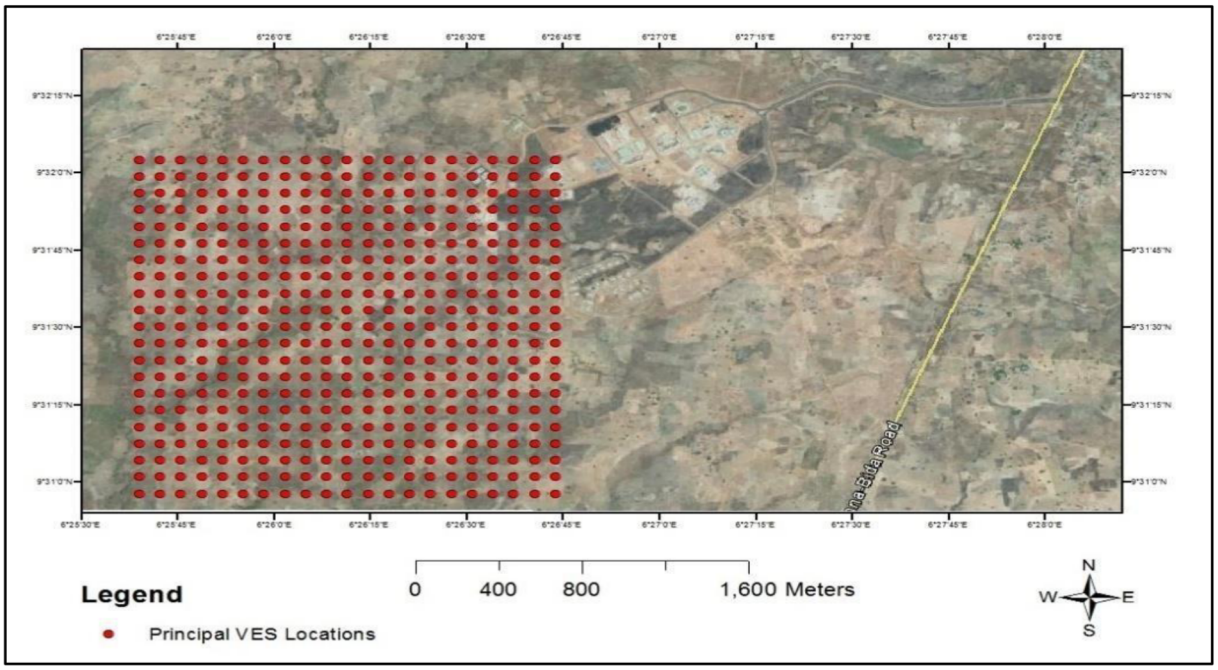

Figure 2. Grid of the 4 km^2 tranche of Phase II Development of the Gidan Kwano Campus at 100 m station-spacing. (The tadpole-shaped feature is Phase I, the present developed portion of the GKC, seen to the northeast of the red-dotted grid of the 4 km^2 areal extent; the Minna-Kateregi-Bida Road is seen as the linear slope to the far east of the grid.)

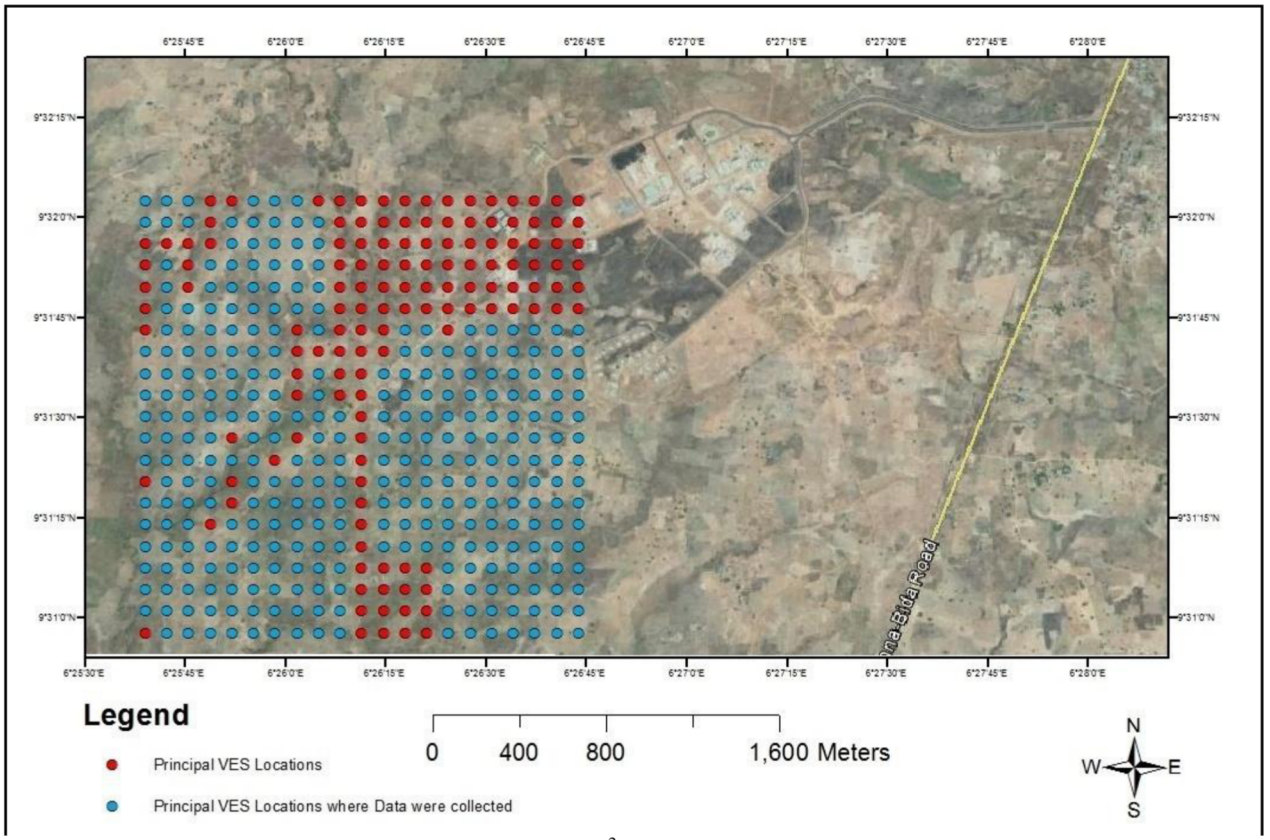

Figure 3. Locations of the principal stations of the 4 km^2 tranche of the Phase II Development colour-coded for locations where data was collected for Jonah and Olasehinde (2017)

The 4 km² survey at the southern Phase II Development was essentially a VES study by design: however, the corresponding IP readings of the VES data-set were also collected to create a huge library of geoelectrical reference data-field; a small-scale self-potential data-field was also acquired in the course of the survey (Jonah and Abdulrasheed, 2018; Jonah and Ibrahim, 2018). The fault-traces of water-bearing fracture signatures inferred from a combination of the geoelectric cross-sections and the induced polarisation tables on the conventional grid matrix of the layout of survey stations for the 4 km²dual VES-IP survey completed at the southern Phase II Development, Gidan Kwano Campus, is represented in Figure 4.

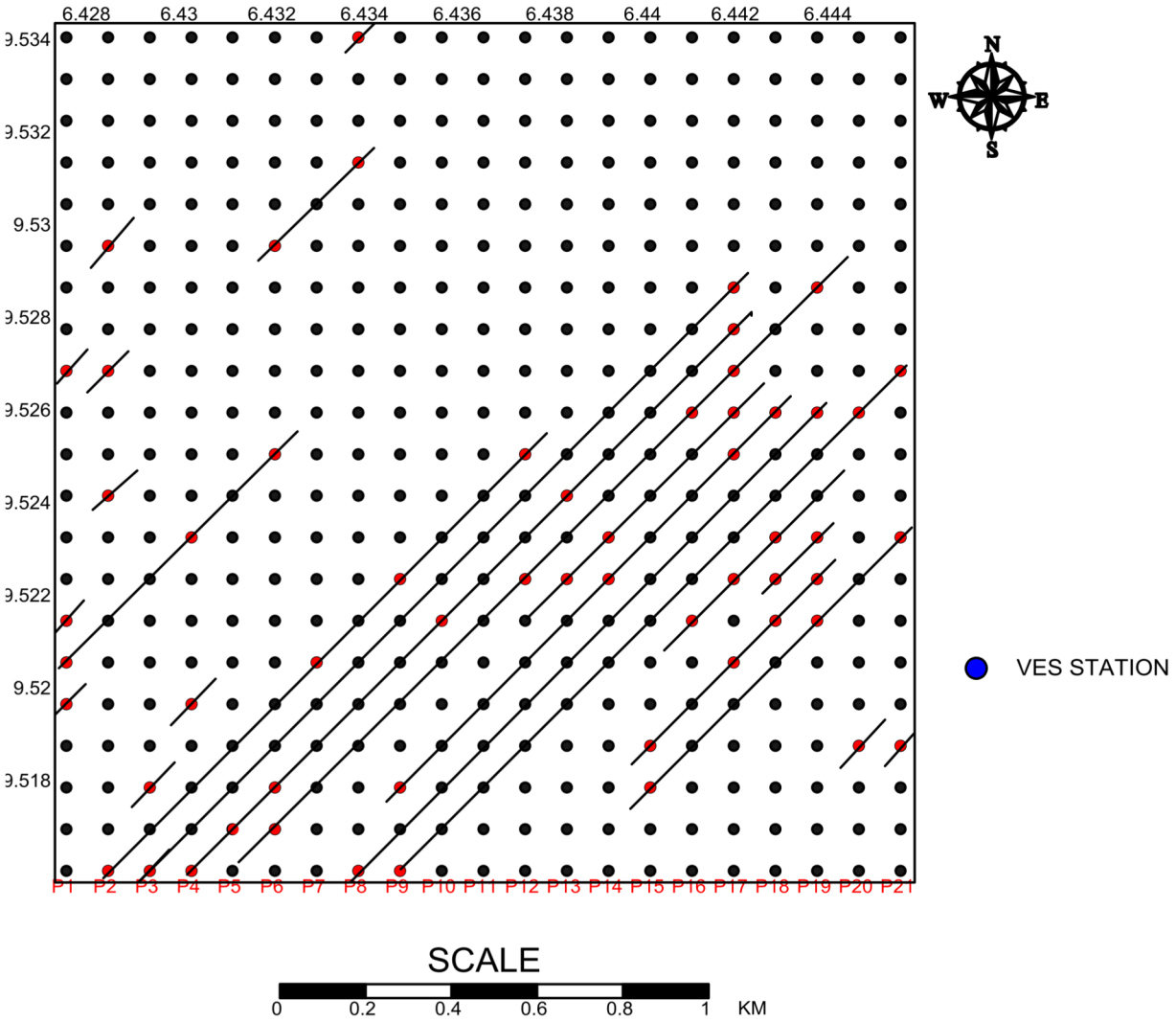

Figure 4. Fault-traces of fracture signatures inferred from a combination of the geoelectric cross-sections and the induced polarisation tables on the conventional grid matrix of the layout of survey stations for the 4 km² (2 km x 2 km) dual VES-IP survey completed at the southern Phase II Development, Gidan Kwano Campus. (The red dots are definite groundwater prospect locations.)

As a result of the arbitrarily-fixed very high correlation threshold chosen for Jonah *et al.* (2018B) which ensured that the method of simple regression analysis was not recommended for geoelectrical surveys at the local basement complex province of the Minna Area even though the fundamental mathematics of this method was sound and the prevailing geology was encouraging, it is still desirable and of utmost importance to further examine the results of the SRA method as applied to the corpus of the 4 km² VES data-field if an agreeable value of the correlation threshold would be chosen. The aim of this study is to expand the scope of Jonah *et al.* (2018B) so as to further examine the results of the SRA method as applied to the corpus of the 4 km² VES data-field for a more agreeable or flexible value of correlation threshold; the key objective of this study is achieved by setting the correlation threshold at the median boundary point of 50%.As a result of the sound mathematical formulations of the method of simple regression analysis and the uniformity of the geology of the area of study over a wide extent with the consideration that Jonah *et al.* (2018B) was a limited-extent test of the validity of using the SRA set at the high boundary point of 75%, it becomes very necessary to re-examine

the fundamentals of the SRA with regards to its application to resistivity surveys. If the planned 841 VES-station survey layout of the wider 8 km^2 Phase II Development were completed, then it would be interesting to test the SRA method for the northern half of this 8 km^2 areal extent where variations and discontinuities in the landform are comparatively sharp.

II. Method

For each groundwater-prospect location, a table of acquired dependent variables (that is, resistivity values) for particular values of the independent variables (that is, AB/2, the current-electrode spacing) was drawn up; such a table is the "x and y table" where x corresponds to AB/2 and y corresponds to the appropriate column of resistivity values. Furthermore, the necessary statistical parameters associated with the SRA method were computed for each table.Subsequently, tables of correlations for the 57 definite groundwater prospect locations down to the 100 m depth-mark and down to the 40 m depth-mark were computed.

III. Result

The acquired resistance values at each survey point out there in the field need to be converted to the true resistivity values of the inhomogeneous earth known as the apparent resistivityvalues; the apparent resistivity value (that is, the resisitivity) for each row was determined by multiplying the acquired resistance value with its corresponding geometric factor.As a result of the considerations presented in Eqs 1 to 3, tables of simple regression analyses were produced, and their abridged format is presented in Appendix A. Subsequently, tables of correlations for the 57 definite groundwater prospect locations down to the 100 m depth-mark and tables of correlations for the 57 definite groundwater prospect locations down to the 40 m depth-mark were produced, and their abridged format is presented in Appendix B. Tables 1 and 2 are the summary tables of percentage conformance medians for the 100m depth-mark and the 40m depth-mark of the preceding simple regression analyses.

Table 1. Summary table of percentage conformance medians for the 100m depth-mark

The 57 definite groundwater prospect locations	**% Conformance Median**
P1-5 ($09^0$31′10.76″; $006^0$25′39.00″)	51.470
P1-6 ($09^0$31′14.00″; $006^0$25′39.00″)	39.859
P1-7 ($09^0$31′17.24″; $006^0$25′39.00″)	83.687
P1-13 ($09^0$31′36.66″; $006^0$25′39.00″)	51.460
P2-1 ($09^0$30′57.80″; $006^0$25′42.24″)	-57.534
P2-10 ($09^0$31′26.96″; $006^0$25′42.24″)	87.085
P2-13 ($09^0$31′36.66″; $006^0$25′42.24″)	83.369
P2-16 ($09^0$31′46.38″; $006^0$25′42.24″)	74.746
P3-1 ($09^0$30′57.80″; $006^0$25′45.48″)	86.839
P3-3 ($09^0$31′04.28″; $006^0$25′45.48″)	80.825
P4-1 ($09^0$30′57.80″; $006^0$25′48.72″)	78.468
P4-5 ($09^0$31′10.76″; $006^0$25′48.72″)	84.260
P4-9 ($09^0$31′23.72″; $006^0$25′48.72″)	88.022
P5-2 ($09^0$31′01.04″; $006^0$25′51.96″)	88.870
P6-2 ($09^0$31′01.04″; $006^0$25′55.20″)	80.513
P6-3 ($09^0$31′04.28″; $006^0$25′55.20″)	74.746
P6-11 ($09^0$31′30.18″; $006^0$25′55.20″)	79.408
P6-16 ($09^0$31′46.38″; $006^0$25′55.20″)	34.593
P7-16 ($09^0$31′14.00″; $006^0$25′58.44″)	11.668
P8-1 ($09^0$30′57.80″; $006^0$26′01.68″)	91.093
P8-18 ($09^0$31′52.86″; $006^0$26′01.68″)	-47.996
P8-21 ($09^0$32′02.58″; $006^0$26′01.68″)	34.799
P9-1 ($09^0$30′57.80″; $006^0$26′04.92″)	31.653
P9-3 ($09^0$31′04.28″; $006^0$26′04.92″)	80.868
P9-8 ($09^0$31′20.48″; $006^0$26′04.92″)	82.930
P10-7 ($09^0$31′17.24″; $006^0$26′08.16″)	88.155
P12-8 ($09^0$31′20.48″; $006^0$26′14.64″)	86.426
P12-11 ($09^0$31′30.18″; $006^0$26′14.64″)	85.334
P13-8 ($09^0$31′20.48″; $006^0$26′17.88″)	63.861
P13-10 ($09^0$31′26.96″; $006^0$26′17.88″)	96.057
P14-8 ($09^0$31′20.48″; $006^0$26′21.12″)	80.641
P14-9 ($09^0$31′23.72″; $006^0$26′21.12″)	-31.767
P15-3 ($09^0$31′04.28″; $006^0$26′24.36″)	75.331
P15-4 ($09^0$31′07.52″; $006^0$26′24.36″)	-38.721
P16-7 ($09^0$31′17.24″; $006^0$26′27.60″)	82.823
P16-12 ($09^0$31′33.42″; $006^0$26′27.60″)	66.456
P17-6 ($09^0$31′14.00″; $006^0$26′30.84″)	50.889
P17-8 ($09^0$31′20.48″; $006^0$26′30.84″)	74.977

P17-11 (09^{0}31′30.18″; 006^{0}26′30.84″)	54.403
P17-12 (09^{0}31′33.42″; 006^{0}26′30.84″)	33.569
P17-13 (09^{0}31′36.66″; 006^{0}26′30.84″)	95.221
P17-14 (09^{0}31′39.90″; 006^{0}26′30.84″)	-13.539
P17-15 (09^{0}31′43.14″; 006^{0}26′30.84″)	86.176
P18-7 (09^{0}31′17.24″; 006^{0}26′34.08″)	73.456
P18-8 (09^{0}31′20.48″; 006^{0}26′34.08″)	83.929
P18-9 (09^{0}31′23.72″; 006^{0}26′34.08″)	-9.553
P18-12 (09^{0}31′33.42″; 006^{0}26′34.08″)	-16.799
P19-7 (09^{0}31′17.24″; 006^{0}26′37.32″)	65.638
P19-8 (09^{0}31′20.48″; 006^{0}26′37.32″)	44.960
P19-9 (09^{0}31′23.72″; 006^{0}26′37.32″)	84.800
P19-12 (09^{0}31′33.42″; 006^{0}26′37.32″)	54.095
P19-15 (09^{0}31′43.14″; 006^{0}26′37.32″)	77.745
P20-4 (09^{0}31′07.52″; 006^{0}26′40.56″)	51.079
P20-12 (09^{0}31′33.42″; 006^{0}26′40.56″)	52.539
P21-4 (09^{0}31′07.52″; 006^{0}26′43.80″)	72.884
P21-9 (09^{0}31′23.72″; 006^{0}26′43.80″)	79.803
P21-13 (09^{0}31′36.66″; 006^{0}26′43.80″)	82.472

Table 2. Summary table of percentage conformance medians for the 40 m depth-mark

The 57 definite groundwater prospect locations	**% Conformance Median**
P1-5 (09^{0}31′10.76″; 006^{0}25′39.00″)	57.493
P1-6 (09^{0}31′14.00″; 006^{0}25′39.00″)	44.209
P1-7 (09^{0}31′17.24″; 006^{0}25′39.00″)	80.732
P1-13 (09^{0}31′36.66″; 006^{0}25′39.00″)	56.353
P2-1 (09^{0}30′57.80″; 006^{0}25′42.24″)	-13.209
P2-10 (09^{0}31′26.96″; 006^{0}25′42.24″)	88.260
P2-13 (09^{0}31′36.66″; 006^{0}25′42.24″)	80.946
P2-16 (09^{0}31′46.38″; 006^{0}25′42.24″)	76.044
P3-1 (09^{0}30′57.80″; 006^{0}25′45.48″)	86.959
P3-3 (09^{0}31′04.28″; 006^{0}25′45.48″)	66.882
P4-1 (09^{0}30′57.80″; 006^{0}25′48.72″)	76.410
P4-5 (09^{0}31′10.76″; 006^{0}25′48.72″)	82.933
P4-9 (09^{0}31′23.72″; 006^{0}25′48.72″)	92.828
P5-2 (09^{0}31′01.04″; 006^{0}25′51.96″)	89.426
P6-2 (09^{0}31′01.04″; 006^{0}25′55.20″)	83.590
P6-3 (09^{0}31′04.28″; 006^{0}25′55.20″)	76.044
P6-11 (09^{0}31′30.18″; 006^{0}25′55.20″)	80.636
P6-16 (09^{0}31′46.38″; 006^{0}25′55.20″)	61.546
P7-16 (09^{0}31′14.00″; 006^{0}25′58.44″)	14.044
P8-1 (09^{0}30′57.80″; 006^{0}26′01.68″)	92.793
P8-18 (09^{0}31′52.86″; 006^{0}26′01.68″)	-59.607
P8-21 (09^{0}32′02.58″; 006^{0}26′01.68″)	30.902
P9-1 (09^{0}30′57.80″; 006^{0}26′04.92″)	38.278
P9-3 (09^{0}31′04.28″; 006^{0}26′04.92″)	81.409
P9-8 (09^{0}31′20.48″; 006^{0}26′04.92″)	84.899
P10-7 (09^{0}31′17.24″; 006^{0}26′08.16″)	83.053
P12-8 (09^{0}31′20.48″; 006^{0}26′14.64″)	86.366
P12-11 (09^{0}31′30.18″; 006^{0}26′14.64″)	84.680
P13-8 (09^{0}31′20.48″; 006^{0}26′17.88″)	72.103
P13-10 (09^{0}31′26.96″; 006^{0}26′17.88″)	96.558
P14-8 (09^{0}31′20.48″; 006^{0}26′21.12″)	85.263

P14-9 (09^{0}31′23.72″; 006^{0}26′21.12″)	1.826
P15-3 (09^{0}31′04.28″; 006^{0}26′24.36″)	84.273
P15-4 (09^{0}31′07.52″; 006^{0}26′24.36″)	-12.989
P16-7 (09^{0}31′17.24″; 006^{0}26′27.60″)	91.664
P16-12 (09^{0}31′33.42″; 006^{0}26′27.60″)	80.864
P17-6 (09^{0}31′14.00″; 006^{0}26′30.84″)	42.849
P17-8 (09^{0}31′20.48″; 006^{0}26′30.84″)	74.579
P17-11 (09^{0}31′30.18″; 006^{0}26′30.84″)	35.080
P17-12 (09^{0}31′33.42″; 006^{0}26′30.84″)	58.918
P17-13 (09^{0}31′36.66″; 006^{0}26′30.84″)	97.085
P17-14 (09^{0}31′39.90″; 006^{0}26′30.84″)	23.843
P17-15 (09^{0}31′43.14″; 006^{0}26′30.84″)	91.166
P18-7 (09^{0}31′17.24″; 006^{0}26′34.08″)	69.893
P18-8 (09^{0}31′20.48″; 006^{0}26′34.08″)	81.709
P18-9 (09^{0}31′23.72″; 006^{0}26′34.08″)	8.094
P18-12 (09^{0}31′33.42″; 006^{0}26′34.08″)	-26.481
P19-7 (09^{0}31′17.24″; 006^{0}26′37.32″)	46.977
P19-8 (09^{0}31′20.48″; 006^{0}26′37.32″)	47.475
P19-9 (09^{0}31′23.72″; 006^{0}26′37.32″)	86.663
P19-12 (09^{0}31′33.42″; 006^{0}26′37.32″)	57.452
P19-15 (09^{0}31′43.14″; 006^{0}26′37.32″)	71.808
P20-4 (09^{0}31′07.52″; 006^{0}26′40.56″)	64.469
P20-12 (09^{0}31′33.42″; 006^{0}26′40.56″)	71.992
P21-4 (09^{0}31′07.52″; 006^{0}26′43.80″)	51.593
P21-9 (09^{0}31′23.72″; 006^{0}26′43.80″)	77.506
P21-13 (09^{0}31′36.66″; 006^{0}26′43.80″)	57.284

IV. Discussion

The choice of the 40 m depth-mark herein is based on the pioneering effort of Jonah *et al.* (2009) in this regard; in that study, the overriding argument for doing simple regression analysis down to the 40 m depth-mark was presented as follows: "*the depth to basement along the profile of the study area is between 26.82 m and 36.79 m (with a mean value of 31.81 m). Furthermore, the study area is just about centrally located in the middle of a large swath of land where information on lithology and depths to basement are readily available from six wells drilled as part of the Petroleum Trust Fund (PTF)-sponsored projects (Jimoh, 1998). In the drilling-for-water report of Jimoh (1998), the well around the School of Environmental Technology (S.E.T.) encountered the basement at about 31 m. The well around the Students' Centre (now Temporary Administration Complex) encountered the basement at 34 m, while the well around the Students' Hostel indicated a depth of 37 m to the basement. Furthermore, the wells drilled around the Staff Quarters, the planned Administration Complex, and Library Complex encountered the basement at depths of 37 m, 34 m, and 31 m. Thus, it means that the six boreholes encountered the fresh basement at an average depth of 34 m, which correlates strong with the result of the Zohdy interpretation. Geological information from Jimoh (1998) indicates that a depth range of 31-34 m is beyond the water-bearing zones characterised by weathered and fractured basement rocks. Thus, as the search for water goes, it is inappropriate to explore beyond 34 m in the core area of study and in the outlying vicinity that could well stretch for over 2 km x 2k m. If this is the case, then the simple regression model could be tested for a maximum depth of AB/2 = 40 m instead of the limit of AB/2 = 100 m that was used in the analysis of...*" Suffice to point out that, several years removed from 2009, the statement concerning the conclusion "thus, as the search for water goes, it is inappropriate to explore beyond 34m in the core area of study and in the outlying vicinity that could well stretch for over 2 km x 2 km" may not be acceptable to all geoscientists working in the local basement complex. In fact, in Jonah *et al.* (2015C and 2015E), the survey crew explored down to the 200 m depth-mark. Nonetheless, in fidelity to the work of Jonah *et al.* (2009), the 40 m depth-depth is being tested herein as a limiting depth of penetration.

The Statistical Weight of the Correlations. For this study, a threshold correlation value between the acquired and predicted values of resistivities (y and y^1)is set at the "fair boundary point"of 50% in order to investigate for an outcome slightly removed from the "tough boundary point" of 75% that was set for the work of Jonah *et al.* (2018B). Overall, positivecorrelation between y and y^1 is achieved, if and only if, there are more threshold correlation valuesgreater than 50% than there are those less than 50% for the 100 m depth mark and for the 40 m depth-mark.

The Statistical Weight of the Correlations for the 100 m Depth-mark:-For the100 m depth-mark, the statistical weight of the correlations of 51.470%:39.859%:83.687%:51.460%:-*57.534%*:87.085%:83.369%:74.746%:86.839%:80.825%:78.468%:84.260%:88.022%:88.870%:80.513%:74.746%:79.408%:34.593%:11.668%:91.093%:*47.996%*:34.799%:31.653%:80.868%:82.930%:88.155%:86.426%:85.334%:63.861%:96.057%:80.641%:*31.767%*:75.331%:*38.721%*:82.823%:66.456%:50.889%:74.977%:54.403%:33.569%:95.221%:*13.539%*:86.176%:73.456%:83.929%:*9.553%*:*16.799%*:65.638%:44.960%:84.800%:54.095%:77.745%:51.079%:52.539%:72.884%:79.803%:82.472 is 42/57th positivecorrelation (or 73.684%). Note that the italiced percentage values are all negative values, as seen in Table 1.

The Statistical Weight of the Correlations for the 40 m Depth-mark:-For the40 m depth-mark, the statistical weight of the correlations of 57.493%:44.209%:80.732%:56.353%:-13.209%:88.260%:80.946%:76.044%:86.959%:66.882%:76.410%:82.933%:92.828%:89.426%:83.590%:76.044%:80.636%:61.546%:14.044%:92.793%:*59.607%*:30.902%:38.278%:81.409%:84.899%:83.053%:86.366%:84.680%:72.103%:96.558%:85.263%:1.826%:84.273%:*12.989%*:91.664%:80.864%:42.849%:74.579%:35.080%:58.918%:97.085%:23.843%:91.166%:69.893%:81.709%:8.094%:*26.481%*:46.977%:47.475%:86.663%:57.452%:71.808%:64.469%:71.992%:51.593%:77.506%:57.284%is 42/57thpositivecorrelation (or 73.684%). Note that the italiced percentage values are all negative values, as well as those values the negative sign is attached, as seen in Table 2.

V. Conclusion

Based on the "fair boundary point" threshold correlation of 50% used for this study, against the "tough boundary point" of 75% that was set for the work of Jonah *et al.* (2018B), a 42/57thor 73.684% positive correlation for y and y^1 of groundwater prospect locations down to 100 m for the 57 definite groundwater prospect locations means that the reliability of the simple regression analysis route is sufficiently excellent to be trusted. Also, based on this 50%threshold correlation, a 42/57thor 73.684% positive correlation for y and y^1 of groundwater prospect locations down to 40 m for the 57 definite groundwater prospect locations means that the simple regression analysis route can be used as a cost-cutting routine whereby maximum depths of survey of intervening prospect locations should be limited to just this 40 m, and then other values downward would be appropriately predicted before inputting into any purpose-specific interpretation software.

VI. Recommendation

It is recommended, henceforth, when working at the local basement province of the Minna Area, to use the simple regression analytical process with acquired geoelectrical data used as a cost-cutting routine whereby maximum depths of survey of intervening prospect locations should be limited to just 40 m, and then other values downward will be appropriately predicted before inputting into any purpose-specific interpretation software.

References

[1]. Akca, I. (2016). ELRIS2D: A MATLAB package for the 2D inversion of DC resistivity/IP data. Acta Geophysica, 64 (2), 443-462.

[2]. Coggon, J.H. (1971). Electromagnetic and electrical modeling by the finite element method. Geophysics, 36(1), 132-155.

[3]. Dey, A. and Morrison, H.F. (1979a). Resistivity modelling for arbitrary shaped two-dimensional structures. Geophysical Prospecting, 27, 1020-1036.

[4]. Dey, A. and Morrison H.F. (1979b). Resistivity modeling for arbitrarily shaped three-dimensional shaped structures. Geophysics, 44, 753-780.

[5]. Jimoh, M.O. (1998). Report on the Six Boreholes Drilled at the Main Campus of the Federal University of Technology, Minna, for the Petroleum (Special) Trust Fund. Cemaco Ventures Ltd., Minna.

[6]. Jonah, S.A. (2016). Analyses of pseudosection specific routes of different orientations of fault-traces to determine groundwater flow pattern at a 4km^2 tranche of New Development, Gidan Kwano Campus Phase II, Federal University of Technology, Minna, Nigeria. Journal of Science, Technology, Mathematics, and Education (JOSTMED), 12(3), 9 - 18.

[7]. Jonah, S.A., Akpomie, D.P., Ezekwebekwe, L. O., Isah, E.A., Muhammed, A.N., Momoh, A.A., Okoye, C.K., Okpara, K. K., Oni, N.O., Alade, R. O., Yahaya, G. A., Zubair, R.O., Onoja, E.U., and Daramola, O. (2015A). A dual topographic-petrographic control for a 1km^2 VES-IP study completed at the Gidan Kwano Campus Phase II Development, Minna, Nigeria. Journal of Science, Technology, Mathematics, and Education (JOSTMED), 11(3), 65 - 76.

[8]. Jonah, S.A. and Abdulrasheed, S. A. (2018). Analysis of self-potential data at a 0.6 km^2 swath of the southern Phase II Development, Gidan Kwano Campus, Minna, northcentral Nigeria. International Journal of Industrial Technology, Engineering, Science, and Education (IJITESED), 1(2), 42 - 49.

[9]. Jonah, S.A. and Adamu, I.B. (2017). Extraction of depth-to-basement information from the interpretation of vertical electrical sounding data of Gidan Kwano Campus Phase II, Federal University of Technology, Minna, Nigeria. Journal of Information, Education, Science, and Technology (JIEST), 4(1), 126 - 132.
[10]. Jonah, S.A. and Ibrahim, M. (2018). Investigation of Patterns of Self-Potential Manifestations across the Southernmost 0.4 km² Tranche of the Phase II Development, Gidan Kwano Campus, Minna, Northcentral Nigeria, BTech Thesis, Federal University of Technology, Minna.
[11]. Jonah, S.A.and Jimoh, M.O. (2016). Validity of an empirical rule for delineating aquifer prospects at the Gidan Kwano Campus Development Phase II, Federal University of Technology, Minna, Northcentral Nigeria. Journal of Science, Technology, Mathematics, and Education (JOSTMED), 12(2), 18 - 24.
[12]. Jonah, S.A. and Olasehinde, P.I. (2015). Qualitative induced polarisation validation of the results of a 2km² VES Study completed at the Gidan Kwano Campus Phase II Development, Federal University of Technology, Minna, Nigeria. Journal of Science, Technology, Mathematics, and Education (JOSTMED), 11(3), 34 - 46.
[13]. Jonah, S.A. and Olasehinde, P.I. (2017). Interpretation of vertical electrical sounding (VES)
[14]. data of Gidan Kwano Campus Phase II, Federal University of Technology, Minna, Nigeria. Journal of Information, Education, Science, and Technology (JIEST), 4(1), 95 - 116.
[15]. Jonah, S.A. and Saidu, S. (2016). On the correlation of area of consistently-low resistivity at depths with slope of the landform of a 4km² tranche of the Gidan Kwano Campus Development Phase II, Federal University of Technology, Minna, Northcentral Nigeria. Journal of Science, Technology, Mathematics, and Education (JOSTMED), 12(2), 34 - 39.
[16]. Jonah, S.A. and Saidu, S. (2018C). Investigation of low-resistivity regimes of the south-central portion of Gidan Kwano (Phase II), Federal University of Technology, Minna, Nigeria. Journal of Information, Education, Science, and Technology (JIEST),5(1), 119-127.
[17]. Jonah, S.A. and Saidu, S. (2018D). Basement aquifer identification from combined topographic, petrological, and resistivity data acquired within FUT's Gidan Kwano Campus, Minna, Northccentral Nigeria. InternationalJournal of Industrial Technology, Engineering, Science, and Education (IJITESED), 1(1), 73 - 80.
[18]. Jonah, S.A. and Saidu, S. (2018E). Correlation of dry season and wet season geoelectrical values for the ABEM Terrameter SAS 4000 at coincident points of measurements. International Journal of Industrial Technology, Engineering, Science, and Education (IJITESED), 1(2), 10 - 22.
[19]. Jonah, S.A., James, G.O., Adeku, D.E., Ahmed, F., Alhassan, A., Hamza, S., Igbideba, O. I., Kwaghhua, F.I., Kyari, M., Macaulay, V. F., Olarewaju, S.I., Onyeodili, G., Popoola, G.B., Sofeso, O.A., Switzer, F.K., and Umoh, U.E. (2015B). Geoelectrical investigation for aquifer and geotechnical properties at the planned Gidan Kwano Campus Development Phase II, Federal University of Technology Minna, Nigeria. Journal of Science, Technology, Mathematics, and Education (JOSTMED), 11(2), 81 - 100.
[20]. Jonah, S.A., Majekodunmi, S.E., Nmadu, E.N., Suleiman, A.O., Muhammad, J.D., and Adamu, I.B. (2018A). Time-lapse agricultural pollution study at a tranche of 4 km² survey at the Gidan Kwano Campus Development Phase II, Minna, Nigeria. Journal of Science, Technology, Mathematics, and Education (JOSTMED), 14(3), 31 - 44.
[21]. Jonah, S.A., Majekodunmi, S.E., Nmadu, E.N., Suleiman, A.O., Muhammad, J.D., and Adamu, I.B. (2018B). Groundwater potential evaluation using simple regression analysis at Gidan Kwano Campus Phase II, Minna, Northcentral Nigeria. Journal of Information, Education, Science, and Technology (JIEST), 5(1), 1-12.
[22]. Jonah, S.A., Olasehinde, P.I., and Umar, M. (2015C). Evaluation of geomorphological quality control of geo-electrical data at Gidan Kwano Campus, Federal University of Technology, Minna, Central Nigeria. Journal of Information, Education, Science, and Technology (JIEST), 2 (1), 122 –134.
[23]. Jonah, S.A., Olasehinde, P.I., Jimoh, M.O., Umar, M., and Yunana, T. (2015D). An intercalated dual geoelectrical survey of an earlier study for groundwater at the planned Gidan Kwano Campus Development Phase II, Federal University of Technology, Minna, Nigeria. Journal of Information, Education, Science, and Technology (JOSTMED), 11(2), 32 - 50.
[24]. Jonah, S.A., Udensi, E.E., Baba-Kutigi A.N., Isah, K.U., Uno, U.E., Ahmadu, U., Crown, I.E., Umar, M.O., Gana, C.S., Kolo, M.T., Rafiu, A.A., Unuevho, C.I., Onoduku, U.S, Abba, F.M., Salako, K.A., Dangana, M.L., Adetona, A.A.,Ibrahim, S.O., Ofor, N.P., Alhassan, D.U., Ezenwora, J. A., Ibrahim, A.G., Eze, C.N., Olarinoye, I. O., Agida, M., Igwe, K.C., Mukhtar, B. and Kimpa, M.I. (2009). The use of a predictive statistical technique in geo-electrical investigations. Journal of Science, Technology, Mathematics, and Education (JOSTMED), 6(2), 136 – 159.
[25]. Koefoed, O. (1979). Geosounding Principles 1: Resistivity Sounding Measurements, Elsevier Science Publishing Company, Amsterdam.
[26]. Loke, M.H. (2001). Tutorial: 2-D and 3-D Electrical Imaging Surveys, Google search, 8th August 2018, 11:08 a.m.
[27]. Morenikeji, W. (2006). Research and Analytical Methods, Jos University Press, Jos
[28]. Mufti, I.R. (1976). Finite-difference resistivity modeling for arbitrarily shaped two-dimensional structures. Geophysics, 41(1), 62-78.
[29]. Pelton, W.H., Rijo,L. and Swift, C.M. (1978). Inversion of two-dimensional resistivity and induced-polarisation data. Geophysics, 43 (4), 788-803.
[30]. Rijo, L. (1977). Modeling of Electric and Electromagnetic Data, PhD Thesis, University of Utah Salt Lake City, USA.

.

Appendix A: Abridged Format of Tables of Simple Regression Analyses for some of the 57 Definite Groundwater Prospect Locations Inferred from Jonah and Olasehinde (2017A)

Table 1. Simple regression analysis table of values for P1-5

x	y	x^2	y^2	Xy	$y-\bar{y}$	$(y-\bar{y})^2$	y^1	$y-y^1$	$(y-y^1)^2$
1.00	39.362	1.000	1549.367	39.362	-218.493	47739.087	71.565	-32.203	1037.036
2.00	28.58	4.000	817.045	57.168	-229.271	52565.082	77.114	-48.530	2355.171
3.00	29.91	9.000	894.728	89.736	-227.943	51957.903	82.663	-52.751	2782.685
5.00	48.767	25.000	2378.220	243.835	-209.088	43717.692	93.761	-44.994	2024.484
6.00	59.291	36.000	3515.423	355.746	-198.564	39427.568	99.310	-40.019	1601.546

6.00	61.27	36.000	3754.013	367.620	-196.585	38645.569	99.310	-38.040	1447.066
8.00	79.648	64.000	2798.410	637.184	-178.207	31757.650	110.408	-30.760	946.204
10.00	103.3	100.000	10670.890	1033.000	-154.555	23887.174	121.507	-18.207	331.478
10.00	82.406	100.000	6790.749	824.060	-175.449	30782.268	121.507	-39.101	1528.853
15.00	148.38	225.000	22016.624	2225.700	-109.475	11984.723	149.252	-0.872	0.760
20.00	234.23	400.000	54863.693	4684.600	-23.625	558.129	176.997	57.233	3275.605
30.00	361.95	900.000	131007.803	10858.500	104.095	10835.819	232.488	129.462	16760.500
40.00	358.83	1600.000	128758.969	14353.200	100.975	10195.999	287.978	70.852	5019.977
40.00	419.8	1600.000	176232.040	16792.000	161.945	26226.260	287.978	131.822	17376.986
50.00	491.49	2500.000	241562.420	24574.500	233.635	54585.424	343.469	148.021	21910.288
60.00	456.06	3600.000	207990.724	27363.600	198.205	39285.316	398.959	57.101	3260.489
70.00	426.41	4900.000	181825.488	29848.700	168.555	28410.868	454.450	-28.040	786.234
80.00	454.23	6400.000	206324.893	36338.400	196.375	38563.234	509.940	-55.710	3103.651
80.00	496.26	6400.000	246273.988	39700.800	238.405	56837.058	509.940	-13.680	187.154
90.00	513.15	8100.000	263322.923	46183.500	255.295	65175.659	565.431	-52.281	2733.300
100.00	521.62	10000.000	272087.424	52162.000	263.765	69572.101	620.922	-99.302	9860.793

Table 2. Simple regression analysis table of values for P1-6

X	y	x^2	y^2	xy	$y-\bar{y}$	$(y-\bar{y})^2$	y^1	$y-y^1$	$(y-y^1)^2$
1.00	178.73	1.000	31944.413	178.730	-25.094	629.702	100.397	78.333	6136.084
2.00	96.974	4.000	9403.957	193.948	-106.850	11416.892	103.478	-6.504	42.297
3.00	66.458	9.000	4416.666	199.374	-137.366	18869.379	106.558	-40.100	1608.046
5.00	52.579	25.000	2764.551	262.895	-151.245	22875.007	112.720	-60.141	3616.947
6.00	56.46	36.000	3187.732	338.760	-147.364	21716.106	115.801	-59.341	3521.338
6.00	51.142	36.000	2615.504	306.852	-152.682	23311.750	115.801	-64.659	4180.769
8.00	65.987	64.000	2798.410	527.896	-137.837	18998.999	121.962	-55.975	3133.254
10.00	85.114	100.000	7244.393	851.140	-118.710	14092.030	128.124	-43.010	1849.867
10.00	72.517	100.000	5258.715	725.170	-131.307	17241.491	128.124	-55.607	3092.148
15.00	119.04	225.000	14170.522	1785.600	-84.784	7188.302	143.528	-24.488	599.667
20.00	153.68	400.000	23617.542	3073.600	-50.144	2514.406	158.932	-5.252	27.585
30.00	243.2	900.000	59146.240	7296.000	39.376	1550.481	189.740	53.460	2857.953
40.00	285.86	1600.000	81715.940	11434.400	82.036	6729.929	220.548	65.312	4265.628
40.00	333.01	1600.000	110895.660	13320.400	129.186	16689.060	220.548	112.462	12647.651
50.00	361.73	2500.000	130848.593	18086.500	157.906	24934.350	251.356	110.374	12182.360
60.00	396.12	3600.000	156911.054	23767.200	192.296	36977.807	282.164	113.956	12985.897
70.00	408.16	4900.000	166594.586	28571.200	204.336	41753.259	312.972	95.188	9060.685
80.00	414.74	6400.000	172009.268	33179.200	210.916	44485.619	343.780	70.960	5035.263
80.00	414.16	6400.000	171528.506	33132.800	210.336	44241.293	343.780	70.380	4953.286
90.00	424.64	8100.000	180319.130	38217.600	220.816	48759.769	374.588	50.052	2505.156
100.00	0.00	10000.000	0.000	0.000	-203.824	41544.165	405.397	-405.397	164346.330

Table 3. Simple regression analysis table of values for P1-7

X	y	x^2	y^2	xy	$y-\bar{y}$	$(y-\bar{y})^2$	y^1	$y-y^1$	$(y-y^1)^2$
1.00	174.68	1.000	30513.102	174.680	-7.270	52.856	39.508	135.172	18271.589
2.00	73.437	4.000	5392.993	146.874	-108.513	11775.113	43.751	29.686	881.286
3.00	39.929	9.000	1594.325	119.787	-142.021	20170.019	47.994	-8.065	65.036
5.00	35.909	25.000	1289.456	179.545	-146.041	21328.029	56.479	-20.570	423.143
6.00	37.415	36.000	1399.882	224.490	-144.535	20890.421	60.722	-23.307	543.236

6.00	36.708	36.000	1347.477	220.248	-145.242	21095.294	60.722	-24.014	576.692
8.00	42.535	64.000	2798.410	340.280	-139.415	19436.595	69.208	-26.673	711.468
10.00	50.21	100.000	2521.044	502.100	-131.740	17355.478	77.694	-27.484	755.387
10.00	61.869	100.000	3827.773	618.690	-120.081	14419.492	77.694	-15.825	250.440
15.00	91.152	225.000	8308.687	1367.280	-90.798	8244.311	98.909	-7.757	60.174
20.00	112.47	400.000	12649.501	2249.400	-69.480	4827.497	120.124	-7.654	58.584
30.00	180.52	900.000	32587.470	5415.600	-1.430	2.045	162.554	17.966	322.786
40.00	202.23	1600.000	40896.973	8089.200	20.280	411.271	204.983	-2.753	7.582
40.00	203.13	1600.000	41261.797	8125.200	21.180	448.584	204.983	-1.853	3.435
50.00	209.04	2500.000	43697.722	10452.000	27.090	733.858	247.413	-38.373	1472.501
60.00	281.43	3600.000	79202.845	16885.800	99.480	9896.233	289.843	-8.413	70.777
70.00	315.96	4900.000	99830.722	22117.200	134.010	17958.629	332.273	-16.313	266.102
80.00	372.92	6400.000	139069.326	29833.600	190.970	36469.468	374.702	-1.782	3.177
80.00	382.89	6400.000	146604.752	30631.200	200.940	40376.807	374.702	8.188	67.038
90.00	432.34	8100.000	186917.876	38910.600	250.390	62695.057	417.132	15.208	231.281
100.00	484.18	10000.000	234430.272	48418.000	302.230	91342.858	459.562	24.618	606.056

Appendix B: Abridged Format of Tables of Correlations for the 57 Definite Groundwater Prospect Locations Down to the 100 m Depth-mark and Down to the 40 m Depth-mark

Table 4. Table of correlation for P1-5 down to the 100m depth-mark

AB/2	Acquired resistivity	Predicted resistivity	Absolute Difference	% Conformance	% Conformance Range	% Conformance Median
1.00	39.362	71.565	32.203	67.797	-48.021	
2.00	28.58	77.114	48.530	51.470	-31.822	
3.00	29.91	82.663	52.751	47.249	-29.462	
5.00	48.767	93.761	44.994	55.006	0.698	
6.00	59.291	99.310	40.019	59.981	29.148	
6.00	61.27	99.310	38.040	61.960	42.767	
8.00	79.648	110.408	30.760	69.240	42.899	
10.00	103.3	121.507	18.207	81.793	44.290	
10.00	82.406	121.507	39.101	60.899	47.249	
15.00	148.38	149.252	0.872	99.128	47.719	
20.00	234.23	176.997	57.233	42.767	51.470	**51.470**
30.00	361.95	232.488	129.462	-29.462	55.006	
40.00	358.83	287.978	70.852	29.148	59.981	
40.00	419.8	287.978	131.822	-31.822	60.899	
50.00	491.49	343.469	148.021	-48.021	61.960	
60.00	456.06	398.959	57.101	42.899	67.797	
70.00	426.41	454.450	28.040	71.960	69.240	
80.00	454.23	509.940	55.710	44.290	71.960	
80.00	496.26	509.940	13.680	86.320	81.793	
90.00	513.15	565.431	52.281	47.719	86.320	
100.00	521.62	620.922	99.302	0.698	99.128	

Table 5. Table of correlation for P1-6 down to the 100m depth-mark

AB/2	Acquired resistivity	Predicted resistivity	Absolute Difference	% Conformance	% Conformance Range	% Conformance Median
1.00	178.73	100.397	78.333	21.667	-305.397	
2.00	96.974	103.478	6.504	93.496	-13.956	
3.00	66.458	106.558	40.100	59.900	-12.462	
5.00	52.579	112.720	60.141	39.859	-10.374	
6.00	56.46	115.801	59.341	40.659	4.812	
6.00	51.142	115.801	64.659	35.341	21.667	
8.00	65.987	121.962	55.975	44.025	29.040	
10.00	85.114	128.124	43.010	56.990	29.620	
10.00	72.517	128.124	55.607	44.393	34.688	
15.00	119.04	143.528	24.488	75.512	35.341	
20.00	153.68	158.932	5.252	94.748	39.859	**39.859**
30.00	243.2	189.740	53.460	46.540	40.659	
40.00	285.86	220.548	65.312	34.688	44.025	
40.00	333.01	220.548	112.462	-12.462	44.393	
50.00	361.73	251.356	110.374	-10.374	46.540	
60.00	396.12	282.164	113.956	-13.956	49.948	
70.00	408.16	312.972	95.188	4.812	56.990	
80.00	414.74	343.780	70.960	29.040	59.900	
80.00	414.16	343.780	70.380	29.620	75.512	
90.00	424.64	374.588	50.052	49.948	93.496	
100.00	0.00	405.397	405.397	-305.397	94.748	

Table 6. Table of correlation for P1-7 down to the 100m depth-mark

AB/2	Acquired resistivity	Predicted resistivity	Absolute Difference	% Conformance	% Conformance Range	% Conformance Median
1.00	174.68	39.508	135.172	-35.172	-35.172	
2.00	73.437	43.751	29.686	70.314	61.627	
3.00	39.929	47.994	8.065	91.935	70.314	
5.00	35.909	56.479	20.570	79.430	72.516	
6.00	37.415	60.722	23.307	76.693	73.327	
6.00	36.708	60.722	24.014	75.986	75.382	
8.00	42.535	69.208	26.673	73.327	75.986	
10.00	50.21	77.694	27.484	72.516	76.693	
10.00	61.869	77.694	15.825	84.175	79.430	
15.00	91.152	98.909	7.757	92.243	82.034	
20.00	112.47	120.124	7.654	92.346	83.687	**83.687**
30.00	180.52	162.554	17.966	82.034	84.175	
40.00	202.23	204.983	2.753	97.247	84.792	
40.00	203.13	204.983	1.853	98.147	91.587	
50.00	209.04	247.413	38.373	61.627	91.812	
60.00	281.43	289.843	8.413	91.587	91.935	
70.00	315.96	332.273	16.313	83.687	92.243	
80.00	372.92	374.702	1.782	98.218	92.346	
80.00	382.89	374.702	8.188	91.812	97.247	
90.00	432.34	417.132	15.208	84.792	98.147	
100.00	484.18	459.562	24.618	75.382	98.218	

Table 7. Table of correlation for P1-5 down to the 40m depth-mark

AB/2	Acquired resistivity	Predicted resistivity	Absolute Difference	% Conformance	% Conformance Range	% Conformance Median
1.00	39.362	71.565	32.203	67.797	-31.822	
2.00	28.58	77.114	48.530	51.470	-29.462	
3.00	29.91	82.663	52.751	47.249	29.148	
5.00	48.767	93.761	44.994	55.006	42.767	
6.00	59.291	99.310	40.019	59.981	47.249	
6.00	61.27	99.310	38.040	61.960	51.470	
8.00	79.648	110.408	30.760	69.240	55.006	**57.493**
10.00	103.3	121.507	18.207	81.793	59.981	
10.00	82.406	121.507	39.101	60.899	60.899	
15.00	148.38	149.252	0.872	99.128	61.960	
20.00	234.23	176.997	57.233	42.767	67.797	
30.00	361.95	232.488	129.462	-29.462	69.240	
40.00	358.83	287.978	70.852	29.148	81.793	
40.00	419.8	287.978	131.822	-31.822	99.128	

Table 8. Table of correlation for P1-6 down to the 40m depth-mark

AB/2	Acquired resistivity	Predicted resistivity	Absolute Difference	% Conformance	% Conformance Range	% Conformance Median
1.00	178.73	100.397	78.333	21.667	-12.462	
2.00	96.974	103.478	6.504	93.496	21.667	
3.00	66.458	106.558	40.100	59.900	34.688	
5.00	52.579	112.720	60.141	39.859	35.341	
6.00	56.46	115.801	59.341	40.659	39.859	
6.00	51.142	115.801	64.659	35.341	40.659	
8.00	65.987	121.962	55.975	44.025	44.025	**44.209**
10.00	85.114	128.124	43.010	56.990	44.393	
10.00	72.517	128.124	55.607	44.393	46.540	
15.00	119.04	143.528	24.488	75.512	56.990	
20.00	153.68	158.932	5.252	94.748	59.900	
30.00	243.2	189.740	53.460	46.540	75.512	
40.00	285.86	220.548	65.312	34.688	93.496	
40.00	333.01	220.548	112.462	-12.462	94.748	

Table 9. Table of correlation for P1-7 down to the 40m depth-mark

AB/2	Acquired resistivity	Predicted resistivity	Absolute Difference	% Conformance	% Conformance Range	% Conformance Median
1.00	174.68	39.508	135.172	-35.172	-35.172	
2.00	73.437	43.751	29.686	70.314	70.314	
3.00	39.929	47.994	8.065	91.935	72.516	
5.00	35.909	56.479	20.570	79.430	73.327	
6.00	37.415	60.722	23.307	76.693	75.986	
6.00	36.708	60.722	24.014	75.986	76.693	
8.00	42.535	69.208	26.673	73.327	79.430	**80.732**
10.00	50.21	77.694	27.484	72.516	82.034	
10.00	61.869	77.694	15.825	84.175	84.175	
15.00	91.152	98.909	7.757	92.243	91.935	

20.00	112.47	120.124	7.654	92.346	92.243
30.00	180.52	162.554	17.966	82.034	92.346
40.00	202.23	204.983	2.753	97.247	97.247
40.00	203.13	204.983	1.853	98.147	98.147

Jonah, S.A, et. al. "Statistical Analysis of Data-set of Groundwater Locations of a 4 km2 VES Data-field at the Southern Phase II Development, Gidan Kwano Campus, Minna, Nigeria." *IOSR Journal of Applied Physics (IOSR-JAP)*, 13(4), 2021, pp. 24-38.